Diffusion and Relaxation in Polymer–Solvent Systems. 1. Poly(*n*-butyl methacrylate)/Methyl Ethyl Ketone

Dou-huong Hwang and Claude Cohen*

School of Chemical Engineering, Cornell University, Ithaca, New York 14853.
Received July 22, 1983

ABSTRACT: Dynamic light scattering experiments provide measurements of binary (mutual) diffusion coefficients. We examine the diffusion and relaxation modes of polymer solutions observed by photon correlation spectroscopy. Unlike simple binary mixtures and dilute polymer solutions, concentrated polymer solutions lead to two binary diffusion coefficients due to the anisotropy of macromolecular diffusion, which accounts for two different mechanisms of concentration fluctuations seen by light scattering in these systems. In this paper we report data on poly(*n*-butyl methacrylate) in methyl ethyl ketone solutions over the entire range of polymer concentration. We complement our binary diffusion coefficient measurements with the self-diffusion of the solvent measured by NMR spin-echo technique.

I. Introduction

It has recently been observed that the photon correlation technique of quasi-elastic light scattering can detect simultaneously with the collective diffusion of segments a "slow" diffusion mode which has been assigned to a variety of mechanisms.[1-4] Both of the observed scattering modes are q^2 dependent, where q is the scattering wave vector. We propose in this paper that the "slow" mode represents a binary diffusion mechanism related to the center-of-mass motion of the macromolecular chains. We shall denote this diffusion by D_{CM} and present in the following section arguments in favor of defining such a diffusion coefficient and why it is different from the self-diffusion of the polymer chains. At very high polymer concentrations and in polymer melts, the photon correlation is typically independent of q and is analyzed in terms of a wide distribution of internal relaxation modes.[5] Near the glass transition of these systems, the slowest internal relaxation time could be in the range of 100 s or longer. Figure 1 is a *schematic* representation of the different dynamic modes observed by light scattering as a function of concentration at a constant temperature. Also indicated on the figure is the window of relaxation times monitored by the photon correlation technique. The behavior of the collective diffusion relaxation $(D_c q^2)^{-1}$ and that of the center-of-mass ("slow") diffusion $(D_{CM}q^2)^{-1}$ presented in Figure 1 are based on extrapolation of our experimental results to be presented below and are also supported by the results of other investigators. The behavior of the slowest internal relaxation mode is drawn according to the relation[6]

$$-[\ln (\tau/\tau_p)]^{-1} = f_2 + f_2^2/\beta\phi_1 \qquad (1)$$

where τ and τ_p are the relaxation times for diluted and pure bulk polymer, respectively; ϕ_1 is the volume fraction of the solvent, and f_2 and β are semiempirical parameters based on Fujita's free volume theory.[7]

The collective diffusion mode is observed only for semidilute and concentrated solutions at concentrations greater than c^*, defined as the concentration at which the macromolecular coils will start to overlap. Although all the experimental evidence points to the fact that the center-of-mass diffusion of the chains in *dilute* solutions goes smoothly into the cooperative diffusion above c^*, we have drawn the D_c curve in Figure 1 starting only above c^* to emphasize that from a theoretical point of view D_c does not exist in dilute solution and one has only D_{CM} in this regime. As indicated in Figure 1, at fairly high polymer concentrations the center-of-mass diffusion will usually be too slow to observe by photon correlation and the observed correlation will represent both the collective diffusion mode and the internal dynamic motion of the chains. Figure 1 is a very schematic representation of the behavior of the slowest modes of macromolecular dynamics as a function of concentration and is intended to be only a useful guide in the data analysis to be reported here on poly(*n*-butyl methacrylate) (PBMA)/methyl ethyl ketone (MEK) systems and in a subsequent paper on poly(methyl methacrylate) (PMMA)/MEK systems. We have attempted to cover the *entire* range of polymer concentration from very dilute solutions to pure melt. Different systems will of course show variations in the relative positions of the three curves of Figure 1; for example, deviation from q^2-dependent diffusion behavior of the correlation function due to q-independent internal relaxation mode will appear at different concentration for different systems. In the PBMA/MEK system the internal motion dynamics of the chains for the molecular weight considered do not couple with the diffusive modes until a very high polymer concentration (~75% by weight) is reached; the analysis of the correlation functions in terms of diffusive q^2-dependent modes below this concentration is then straightforward. For the PMMA/MEK system, coupling between the collective diffusion and the internal dynamics occurs at the lower polymer concentration of 55% and the more complex analysis of the correlation function in terms of this coupling (which leads to a non q^2 dependence of the relaxation time) will be presented in a following paper presenting the results on that system. We have also complemented our light scattering data with pulsed-gradient spin-echo NMR measurements of the self-diffusion coefficient D^*_s of the solvent MEK.

Since there has been some confusion with regard to what is the character of the slow diffusion mode observed by light scattering, we briefly digress in the following section to describe the nature of the various diffusion coefficients measured in entangled polymer solutions before turning to the experimental section and the discussion of our results.

II. Diffusion Coefficients in Entangled Polymer Solutions

There has been some confusion, albeit a controversy, with regard to what is the character of the "slow" diffusion mode observed by light scattering.[1-4] The dynamic light scattering experiments, which are based on the refractive index difference between the two components of a binary mixture, measure *mutual* diffusion coefficients in a frame of reference relative to the mean-volume velocity and not the self-diffusion coefficient unless the results are extrapolated to infinite dilution. At any finite concentration, the diffusion observed by light scattering will be different

0024-9297/84/2217-1679$01.50/0

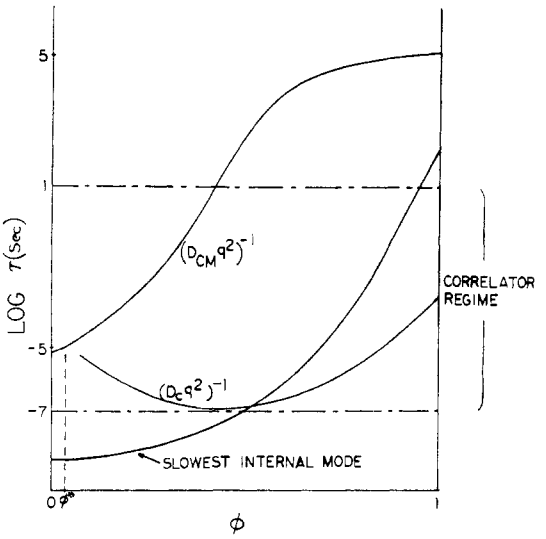

Figure 1. Schematic representation of relaxation times of various modes vs. polymer concentration. On the right ordinate the window accessible to the photon correlation experiment is indicated.

from that observed by monitoring the motion of tagged particles by techniques such as NMR and forced Rayleigh scattering because purely thermodynamic interaction terms (and not only a frictional term) enter in the definition of binary diffusion coefficient seen by light scattering.[8] In entangled polymer solutions there are two different mechanisms for the change of concentration in a given thermodynamic system: one mechanism corresponds to the swelling or deswelling of the system, with the topology of the polymer network remaining unchanged, and the other corresponds to a change of concentration due to center-of-mass motion (reptation-like at high polymer concentration) of macromolecular chains into or out of the system. Both mechanisms occur in concentrated polymer solutions but only the first mechanism is permitted in a permanently cross-linked polymer network (gel). The physical reason for the two mechanisms in solutions is intimately tied to the anisotropic nature of the diffusion of the macromolecular chains past the overlap concentration c^*. Below c^*, D_{CM} is isotropic; but beyond c^* and more clearly in entangled solutions, the motion of sections of the chain between entanglements which leads to the collective diffusion D_c can be thought as being primarily in a direction perpendicular to the line between entanglements, whereas the slow-mode D_{CM} is essentially due to a motion parallel to the chain backbone. Between c^* and the concentration at which entanglements clearly set in (c^{**} or c_e), these two modes will probably be coupled as their time scales are quite close; there is evidence, for example, that in this region D_c is not independent of molecular weight[9,10] as it should be in theory.[11] Obviously if a continuous line is drawn through the data of D_c encompassing the data in the *dilute* regime, there will be a transition region where D_c will depend on molecular weight as the two modes merge below c^*. The general statement that diffusion in any two-component mixture can be described by a single mutual (or binary) diffusion coefficient which may be a function of composition but will be the same for both components will not hold for entangled polymer solutions. Bearman in 1961 in his statistical mechanical formulation of diffusion coefficients had already cautioned about this point.[12] In a frame of reference fixed relative to the mean-volume velocity, the mutual diffusion coefficients in a two-component system can be expressed as[12,13]

$$D_{12} = \frac{c_1\bar{v}_2}{\xi_{12}}\left(\frac{\partial\mu_1}{\partial c_1}\right)_{T,P} \tag{2a}$$

$$D_{21} = \frac{c_2\bar{v}_1}{\xi_{21}}\left(\frac{\partial\mu_2}{\partial c_2}\right)_{T,P} \tag{2b}$$

where c_i, $\bar{v}_i$, and μ_i are the concentration, partial volume, and chemical potential of component i and ξ_{ij} is the coefficient of friction of i in j. Only in binary mixtures of simple liquids when the pair interaction potential between a molecule 1 and a molecule 2 may be regarded as a smoothed potential in which the effects of orientation and internal degrees of freedom have been *averaged out* will ξ_{12} equal ξ_{21} and thereby D_{12} equal D_{21}, leading to a single diffusion coefficient.[12] This situation holds for dilute polymer solutions (below the overlap concentration c^*) and when the volume of the thermodynamic system considered is very large compared to the macromolecular size. Above c^*, however, ξ_{12} will differ from ξ_{21}, and $D_{12} \neq D_{21}$. Unlike simple binary mixtures and dilute polymer solutions, which are characterized by a single binary diffusion coefficient, entangled polymer solutions will lead to two binary diffusion coefficients observable by light scattering. One coefficient has been associated with the collective diffusion of segments, and the other is associated with the center-of-mass motion of the polymer molecules. Stated differently, the center-of-mass diffusion which is random and isotropic in dilute solutions is breaking into two components beyond c^* due to the anisotropy of the diffusion process. One can also define self-diffusion coefficients for the two components in the mixtures by defining the friction factors[12,14]

$$\xi_1 = c_1\xi_{11} + c_2\xi_{12} \tag{3a}$$

$$\xi_2 = c_2\xi_{22} + c_1\xi_{21} \tag{3b}$$

where ξ_1 will lead to a self-diffusion coefficient for the solvent molecules D_s^* and ξ_2 will lead to a self-diffusion coefficient for the polymer molecules D_p^*. These coefficients are not affected by thermodynamic interactions in the form of second and higher virial coefficients arising from $\partial\mu/\partial c$ in eq 2,[8] and there lies the difference between D_p^* and D_{CM}. In an entangled polymer system one can then determine *four* experimental diffusion coefficients: D_c, D_{CM}, D_s^*, and D_p^*. We report measurements of D_c, D_{CM}, and D_s^* in PBMA/MEK systems of a wide range of concentration.

III. Experimental Section

A. Samples for Light Scattering. (1) Solutions with Less Than or Equal To 40% by Weight Polymer. Linear poly(*n*-butyl methacrylate) was prepared by suspension polymerization initiated by benzoyl peroxide at 70 °C. The polydispersity and the molecular weight of the polymer were determined by gel permeation chromatography (GPC). The weight-average molecular weight M_w was determined to be 4.5×10^5 and the polydispersity index M_w/M_n was ~3. The polymer was dissolved in methyl ethyl ketone predistilled over CaH_2. Polymer solutions (except the 40% samples) were filtered through 0.22-μm Teflon membrane filters directly into cylindrical scattering cells (i.d. = 13 mm). The 40% solution was obtained by evaporation of a 30% solution in a vacuum oven. Solutions were freed from dust by centrifugation for 2 h at 15000g, where g is the gravitational acceleration.

(2) Highly Concentrated Solutions (≥55%). These polymer solutions were prepared directly in the scattering cells from monomer (BMA)–solvent (MEK) mixtures. The monomer was put into a tube that was connected to the vacuum distillation and degassing setup shown in Figure 2 and was dehydrated with CaH_2 for 3 days with mixing. The monomer was degassed by the freeze–thaw technique for several cycles until no further evolution

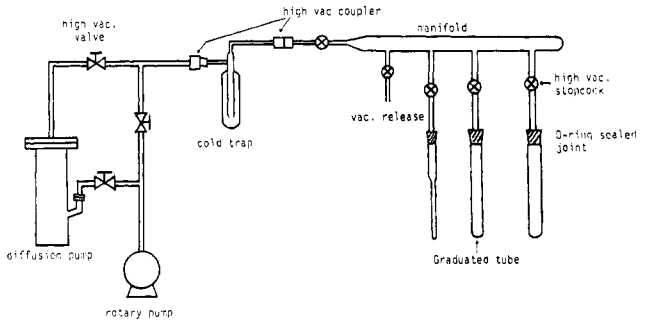

Figure 2. Vacuum distillation and degassing setup for the preparation of highly concentrated solutions and polymer melts.

of gas occurred while thawing, then vacuum distilled into a graduated tube, and warmed to room temperature. This procedure was repeated separately for the solvent. The required amount of monomer was vacuum distilled again into a necked light scattering cell that contained benzoyl peroxide (0.1% of final composition) and *tert*-butyl hydroperoxide (0.05%). The latter was used to ensure completion of polymerization. Subsequently, the appropriate amount of solvent was distilled into the same cell, and the cell was flame-sealed under vacuum. The mixture was centrifuged at 15000*g* for 1 h to deposit any dust particles that may have escaped all previous precautions at the bottom of the cell. The monomer was polymerized at 90 °C for 1 day and then kept in an oven at 140 °C for 1 week to drive the reaction to completion. All samples were left at 40 °C for 1 week, and the temperature was then gradually brought down to room temperature. The weight-average molecular weight and polydispersity index of the 55%, 65%, and 100% samples were respectively 3.2 × 10^5, 3.6 × 10^5, and 9.7 × 10^5 and 1.7, 1.6, and 3. Locally, in the preparation tube, the pure bulk polymer had a polydispersity of about 1.7. There was, however, a molecular weight gradient toward the center, owing, we believe to wall effects and temperature gradient that lead to an overall polydispersity of close to 3.

B. Light Scattering Setup. A Lexel 85 argon ion laser (λ = 4880 Å) was used in conjunction with a photomultiplier tube (EMI9789A) and a Birnboim correlator (Data Acquisition System, DAS III, Science Research Systems of Troy, Troy, NY). A temperature-controlling bath and jacket for the sample holder allowed temperature regulation from −30 to approximately +100 °C to better than ±0.1 °C. All the experiments reported here were performed at 19 °C except when otherwise indicated.

C. Proton NMR. (1) Materials. Linear poly(*n*-butyl methacrylate) was prepared by solution polymerization in MEK at 60 °C with benzoyl peroxide as initiator. The value of M_n was determined by GPC to be 90 000 and the polydispersity ratio was ~1.5. Low-concentration samples (≤40% by weight polymer) were obtained by dissolving appropriate amounts of precipitated polymer into the solvent MEK; the solutions were then transferred into NMR microcells. Higher concentrations were prepared by evaporation of a 50% solution in a vacuum oven.

(2) Measurement of Self-Diffusion of Solvent. The pulsed-gradient spin-echo measurements of solvent self-diffusion were performed at 79.54 MHz by using the Carr–Purcell pulse sequence. Experiments were made on a CFT-20 Varian NMR spectrometer at 26 °C. In order to avoid the signal contribution due to the polymer, the delay time τ between 90° and 180° radio-frequency pulses (and hence the effective diffusion time) was 40–180 ms. The field gradient G was ~0.4 G/cm, and D_2O was used for lock purposes. For comparison with light-scattering measurements at 19 °C, the NMR self-diffusion values were assumed to be inversely proportional to temperature, which is a reasonable approximation in view of the closeness of the two temperatures.

IV. Analysis of the Time-Correlation Function

The normalized intensity autocorrelation function in a homodyne experiment for a single-relaxation process of amplitude A and decay constant Γ can be expressed as[15]

$$g_{HO}^{(2)}(t) = 1 + Ae^{2\Gamma t} \quad (4)$$

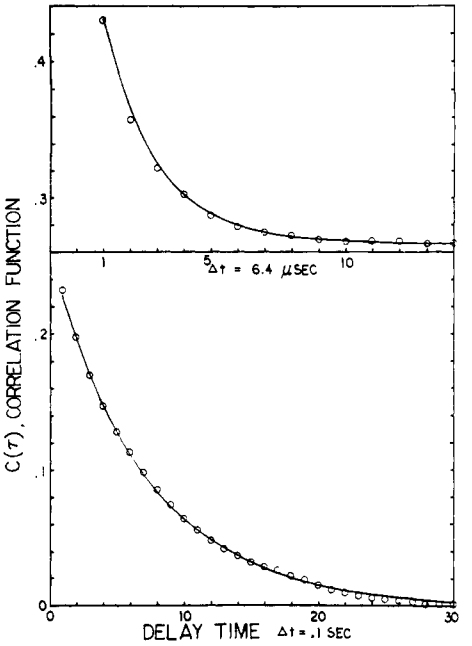

Figure 3. Plots of the correlation functions for 30% PBMA in MEK at a scattering angle of 60° for two widely different delay times. The top figure is for the fast diffusion and the bottom one for the slow diffusion. Each curve is a single-exponential fit to the data points.

For the heterodyne experiment, the intensity autocorrelation is given by[15]

$$g_{HE}^{(2)}(t) = 1 + Ae^{-\Gamma t} \quad (5)$$

The experimental photon correlation function $C(t)$ is identified with $g^{(2)}(t)$ within a constant nonzero term.[16] In the event of two simultaneous relaxation processes, the correlation function becomes

$$g^{(2)}(t) = 1 + (A_f e^{-\Gamma_f t} + A_s e^{-\Gamma_s t})^2 \quad (6)$$

where A_s and A_f and Γ_f are the amplitudes and decay constants of the slow and fast relaxation processes, respectively.

Amis et al.[3b] have proposed that provided the fast and slow processes give rise to a weak and strong scattering amplitude, respectively, and that the two processes are well separated in time scale, the fast process is detected by heterodyne scattering whereas the slow process is detected by homodyne scattering. They reported that even with an intensity ratio A_s/A_f as low as 1.5, use of the heterodyne detection scheme for the fast process was the more appropriate approach for their results. By examining the various contributions to our intensity correlation function, we indeed reach a similar conclusion.[17] We have therefore followed their proposed procedure and fitted our scattering data for 20% and 30% solutions using eq 4 for the slow diffusion relaxation mode. Values of A_s and Γ_s were thus extracted from the correlation functions with long delay times. The fast diffusion process was then fitted to a correlation of the form

$$C(t) = B + A_f e^{-\Gamma_f t} \quad (7)$$

where B was a floating base line. Figure 3 shows the fast and slow correlation functions for 30% PMBA in MEK. The required delay times for these correlations were separated by 4 orders of magnitude. Intensity correlations from the less concentrated solutions were analyzed on the basis of homodyne scattering (eq 6). Again, A_s and Γ_s were first obtained from the long delay time correlation function. For the highly concentrated solutions (55% and

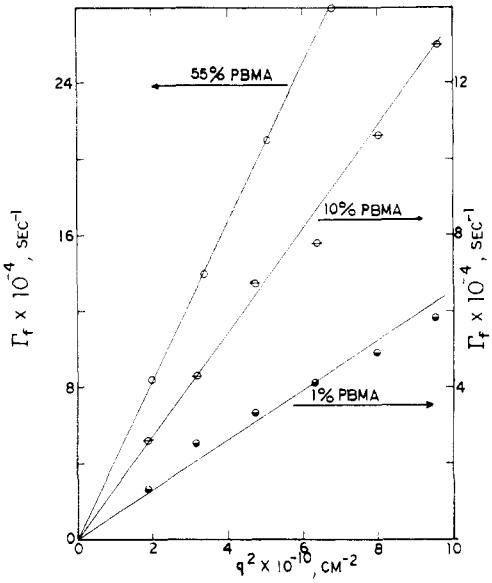

Figure 4. Plots of Γ_f (fast) vs. q^2 for solutions of 1, 10, and 55 wt % polymer.

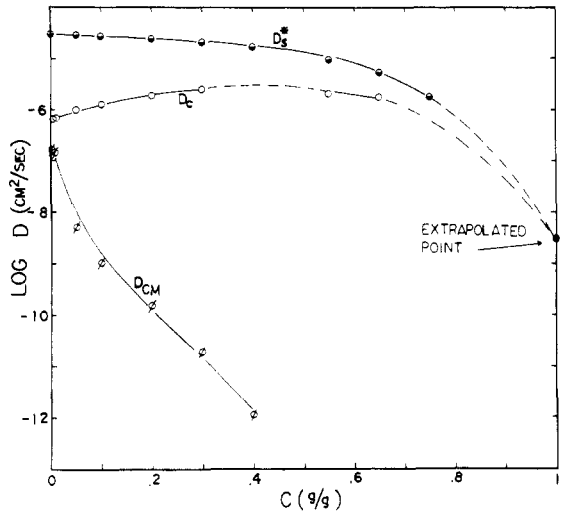

Figure 5. Diffusion coefficients vs. concentration for PBMA/MEK at 19 °C. D^*_s is the self-diffusion of MEK obtained by NMR at 26 °C and reduced to 19 °C. D_c, the cooperative diffusion coefficient, and D_{CM}, the center-of-mass diffusion coefficient, are "binary" diffusion coefficients obtained by photon correlation for $c > c^*$.

65%), the slow diffusion process was not detected within the time limit of the correlator and since the total scattered intensity of these solutions was low (about the same as the 1% solution), it was more appropriate to use the homodyne analysis in the absence of strong local oscillators.

V. Results and Discussion

A. Cooperative Diffusion. Figure 4 illustrates the typical q^2 dependence of the fast decay constant. Because of the shortest delay time limitation of our software correlator, some of the fast signals at high angles (greater than 90°) were not successfully detected. Similarly, because the cooperative diffusion coefficient D_c increases initially with concentration was shown in Figure 5, its corresponding decay time in the 40% solution becomes too fast to be monitored by our correlator. The data points for D_c and D_{CM} reported in Figure 5 are only for $c > c^*$. The diffusion below c^* (in the dilute regime) leads to a single exponential, which we have found more natural to link to the "slow" mode (D_{CM}) above c^* as reported in Figure 6, although as discussed earlier, D_c and D_{CM} merge below c^*. The co-

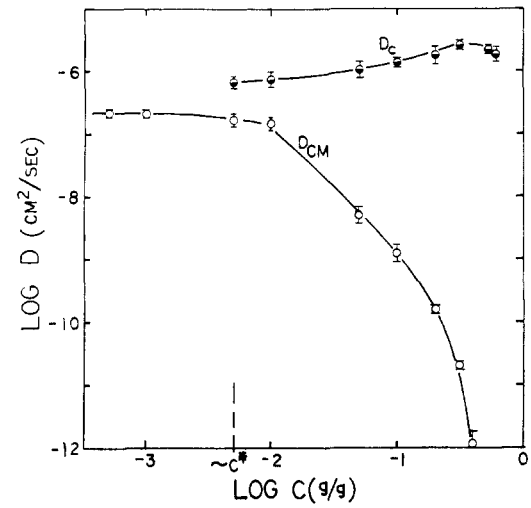

Figure 6. Logarithmic plot of D_c and D_{CM} vs. concentration. In the semidilute regime a 0.3 scaling exponent is obtained for D_c and an exponent of −2 for D_{CM}.

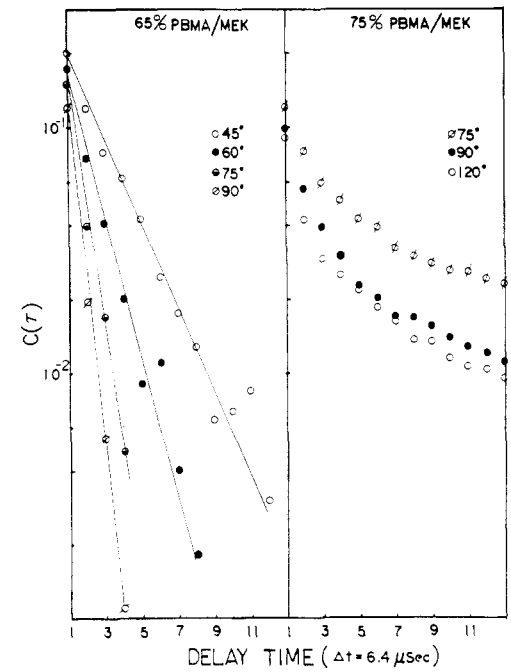

Figure 7. Correlation functions at different angles for 65% and 75% PBMA in MEK.

operative diffusion goes through a maximum and decreases at high concentrations where it was measured for 55% and 65% solutions. Above 65% it was impossible to detect the q^2 dependence of the relaxation frequency. This is illustrated in Figure 7, which shows that the 65% solution gives an exponential decay of the fast component of the correlation function over approximately 2 orders of magnitude. For the 75% solution, on the other hand, no exponential decay was observed and the decay exhibits an angular dependence that becomes weaker at higher angles. In terms of Figure 1, we have surpassed the intersection of $(D_c q^2)^{-1}$ and the slowest internal mode curves, which occurs between 65% and 75% polymer in the PBMA/MEK system. The internal mode distribution of relaxations has overtaken the fast portion of the correlation and the cooperative diffusion mode now is inextricably coupled to internal relaxation modes that are faster than the slowest mode. This coupling leads to what is commonly called "anomalous" or non-Fickian diffusion observed in classical diffusion experiments in polymers.[18] We note that

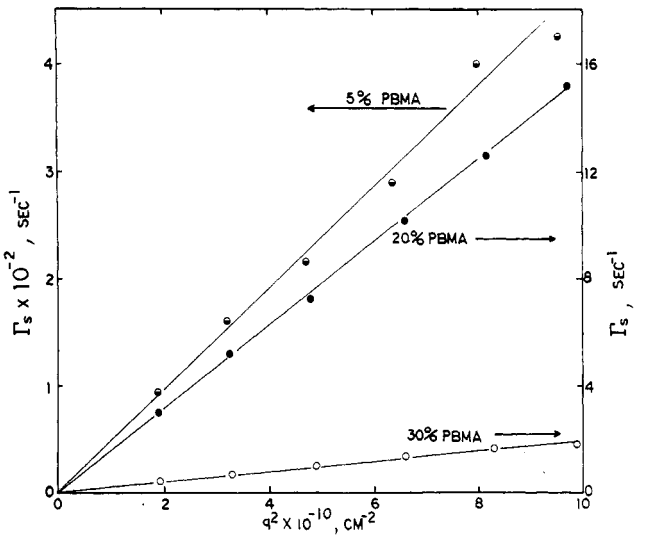

Figure 8. q^2 dependence of Γ_s (slow) for three different solutions.

"anomalous" diffusion is usually observed only below the glass transition where the internal relaxations are very slow; but in this case the diffusion experiments are performed on a macroscopic length scale L such that the diffusion time $(D/L^2)^{-1}$ is again comparable to internal relaxation times when the anomaly (i.e., coupling) occurs.[19] In dynamic light scattering the length scale over which diffusion is probed is the inverse scattering wave vector and Dq^2 is comparable to internal relaxation frequencies far above the glass transition and for a substantially diluted polymer (75% PBMA in MEK for the case under consideration). The initial slope of the correlation function for the 75% solution shown in Figure 7 is not q^2 dependent because $(D_c q^2)^{-1}$ is no longer the fastest relaxation time observed. Accordingly, it will be impossible to extract D_c from the shape of the correlation, and a different analysis of the correlation to be presented later is required.

The cooperative diffusion coefficient D_c can only be observed at concentrations beyond the minimum overlap concentration c^*, which is ~0.5% in our PBMA/MEK system. Below that concentration, only the center-of-mass diffusion D_{CM} of independent polymer molecules in dilute solutions is observed as indicated in Figure 6. In the semidilute regime ($c \geq 0.5\%$) we observe for D_c a power law index of approximately 0.30, which increases at higher concentrations (Figure 6). The scaling prediction for the cooperative diffusion coefficient D_c^s defined in a frame of reference relative to the *solvent velocity*[11] gives a power law with an exponent of 0.75 in the semidilute regime. To compare with the scaling law prediction one should therefore transform the light scattering values of D_c measured in a frame of reference relative to the *volume velocity*. The two diffusion coefficients are related by[20] $D_c = D_c^s(1 - \phi_2)$, where ϕ_2 is the volume fraction of the polymer. We find that in the region just above $c = 0.5\%$, the exponent for D_c^s is ~0.4. Other workers have reported similar discrepancies from the scaling prediction for other systems.[3] The limiting value of D_c at zero solvent concentration shown in Figure 5 was obtained by extrapolation of the NMR solvent self-diffusion measurements since it is expected that in the limit of $\phi \to 1$, $D_c = D_s^*$. The details of the extrapolation procedure are discussed in section C.

B. Center-of-Mass Diffusion. Figure 8 shows that the relaxation frequencies Γ_s of the slow decay mode obtained with long delay times are indeed q^2 dependent within experimental errors. The diffusion coefficients D_{CM} $(=\Gamma_s/q^2)$ which we have associated with the binary center-of-mass diffusion of the polymer chains are listed in Table I along with values of D_c and D_s^*. Figures 5 and 6 show as anticipated a very rapid decrease of D_{CM} with concentration above $c \sim 1\%$. The behavior of the D_{CM} curve in Figure 6 exhibits the drastic change in the nature of the center-of-mass diffusion of the chains as a function of concentration. The random Brownian behavior of the individual macromolecular particles at $c < 0.5\%$ is replaced by the much slower reptative-like motion at high polymer concentrations. At concentration higher than 55%, the center-of-mass diffusion becomes too slow to be detectable with our correlator. In the concentration regime just above 1% (semidilute regime), our results for D_{CM} can be described by a scaling law with an exponent of −2.0. It is obvious from Figure 6 that even more so than the results for D_c, the power of the exponent here is a strong function of the concentration. It should be pointed out, however, that the scaling prediction of an exponent of −1.75 is for the self-diffusion of the polymer chain D_p^* and not for the binary diffusion D_{CM} observed by light scattering. Leger et al.[21] have demonstrated for example that D_p^* measured by forced Rayleigh scattering on polystyrene/benzene solutions is in good agreement with scaling and reptation predictions over a fairly wide concentration range.

Table I
Values of D_s^*, D_c, and D_{CM} in PBMA/MEK Systems

w, g/g %	$D_s^{*26°C}$, cm^2/s	$D_c^{19°C}$, cm^2/s	$D_{CM}^{19°C}$, cm^2/s
0	3.11×10^{-5}		
0.05			2.14×10^{-7}
0.01			2.10×10^{-7}
0.5		6.75×10^{-7}	1.64×10^{-7}
1		6.84×10^{-7}	1.47×10^{-7}
5	2.99×10^{-5}	1.00×10^{-6}	4.77×10^{-9}
10	2.77×10^{-5}	1.34×10^{-6}	1.18×10^{-9}
20	2.42×10^{-5}	1.76×10^{-6}	1.55×10^{-10}
30	2.16×10^{-5}	2.42×10^{-6}	2.00×10^{-11}
40	1.74×10^{-5}		1.13×10^{-12}
55	9.24×10^{-6}	2.08×10^{-6}	
65	5.30×10^{-6}	1.76×10^{-6}	
75	1.90×10^{-7}		
100	2.96×10^{-9} [a]		

[a] Obtained from extrapolation.

In simple binary mixtures, it is usually expected that the mutual diffusion coefficient is smaller than the self-diffusion coefficient of the fast-moving component and greater than that of the slow-moving component.[22] In dilute polymer solutions (below c^*) where we have isotropic macromolecular diffusion leading to a single mutual diffusion coefficient, this appears to be indeed so.[23] Above c^*, however, the presence of two binary diffusion coefficients appears to complicate things as Chang and Yu[3c] have reported measurements of D_p^* that are greater than D_{CM} and lower than D_c. An intersection (crossover) of the two curves for D_p^* as a function of concentration might therefore be occurring at $c \sim c^*$. More work will be needed to illustrate this interesting feature. We note that D_p^* and D_{CM} are identical in the limiting cases of $\phi_2 \to 0$ and of $\phi_2 \to 1$ if we assume that $\xi_{21} = \xi_{22}$ in that limit. In Figure 9 we show the ratio of the amplitude of the slow diffusion mode to that of the fast diffusion mode. As has been previously reported on other systems[1,24] this ratio decreases drastically as the polymer concentration decreases with higher amplitude ratios observed at lower scattering angles. As the density of entanglements decreases, the amplitude of the collective or fast motion primarily perpendicular to the line between entanglements increases due to the decrease of constraints. The observed angular dependence implies that at small angles one increases the chances of observing the slow diffusion along the chain. We note also

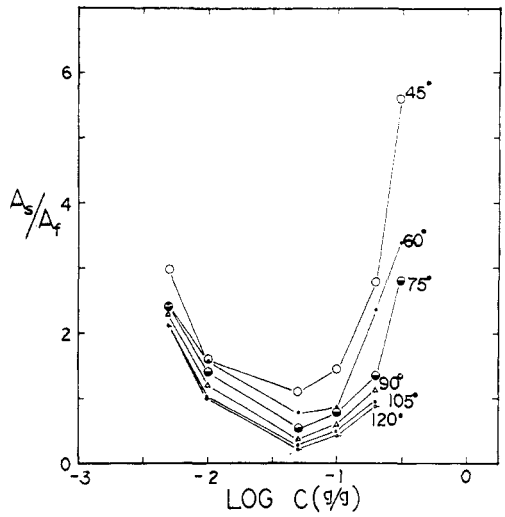

Figure 9. Plot of the amplitude ratio of the slow to the fast modes vs. concentration at various angles.

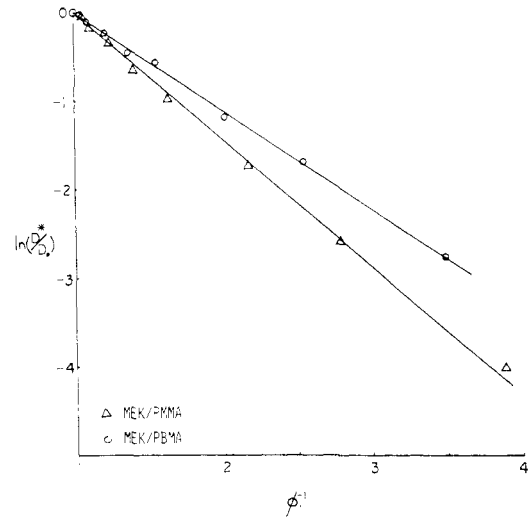

Figure 10. Plot of ln (D^*/D_0) vs. ϕ_1^{-1} for MEK in PMMA (△) and in PBMA (○). The curves are best fit straight lines to the experimental data.

that as the concentration of polymer is decreased even further, the amplitude ratio turns around and goes up again. This is linked to the fact that the overlap probability of polymer coils is diminishing as the number density of coils drops and we approach c^* from above. Obviously below c^* the center-of-mass translation diffusion dominates the scattering amplitude since the cooperative (fast) diffusion mode contribution has altogether vanished.

C. Solvent Self-Diffusion. The decrease in the value of the self-diffusion coefficient of a solvent due to the presence of a polymer in a solution or a gel has been interpreted with some limited success in terms of the obstruction theory and its modifications.[25] At the other end of the concentration spectrum, i.e., for plasticized polymer melts, the modified free volume model due to Fujita[5] is successful in describing the mutual diffusion for many polymer/organic diluent systems at very high polymer volume fraction. Recent versions of the free volume approach due to Vrentas and Duda[26] and to Paul[27] attempt to improve this situation and to produce a predictive version of the free volume theory.

We have found that the self-diffusion coefficient D_s^* of MEK presented in Table I and obtained by the NMR pulse-gradient spin-echo technique in the systems MEK/PBMA and MEK/PMMA follow surprisingly well the simple relation

$$\ln (D_s^*/D_0) = B_0(1 - B/B_0\phi_1)/v_f(T,0) \qquad (8)$$

where D_0 is the self-diffusion of pure MEK, B is a constant representing a measure of the critical size "hole" necessary in order for a diffusion jump of the solvent molecule to occur, B_0 is the value of B in pure solvent, ϕ_1 is the volume fraction of solvent, and $v_f(T,0) = v_f(T,\phi_2 = 0)$ is the fractional free volume of the pure solvent at temperature T. Equation 8 can be obtained from a generalized Doolittle empirical expression for the self-diffusion of small molecules[28]

$$D_s^* = A \exp[-B/v_f(T,\phi_1)] \qquad (9)$$

by assuming that the addition of a polymer to the solvent decreases the fractional free volume v_f available to solvent diffusion. The prefactor A in eq 9 depends primarily upon the size and shape of the solvent molecule. Equation 8 follows immediately from (9) if one assumes that the constant B is only weakly dependent on the concentration of the system and that the fractional free volume contribution of the solvent is much greater than that of the polymer.[29] Obviously the latter assumption will break down at very high polymer concentration where the fractional free volume contribution of the polymer becomes significant and where Fujita's approach is successful, but in the remaining very wide range of polymer concentration (ϕ_2 from 0 to 0.75 for our data on MEK/PMMA) this assumption appears legitimate, as demonstrated by the validity of eq 8 in Figure 10. We note that the constant B representing the slopes of the lines in Figure 10 is different for the same solvent (MEK) in different polymers, indicating that B is not equal to B_0 and that it must somehow incorporate the different molecular interactions of MEK/PBMA and MEK/PMMA. We have also tested eq 8 with previously reported data of self-diffusion coefficients of water in polyacrylamide solutions and gels,[30] of water in dextran solutions,[25] and of a third solute in the polymer solutions.[17] The inverse proportionality between ln (D_s^*/D_0) and ϕ_1 is well obeyed in all the cases considered. The values of B for the self-diffusion of water in polyacrylamide solutions and in dextran solutions are practically equal,[17] suggesting that the strong hydrogen-bonding character of the water molecules may be the dominating factor in the molecular interactions in these systems. In terms of Vrentas and Duda's extension of the free volume approach, this last result would indicate that polyacrylamide, a linear aliphatic molecule, has the same jumping unit as dextran with its heterocyclic segments. Since this appears unlikely, it is suggested that the effect of the interaction between solvent and polymer (strong H bonding in this case) built into the empirical constant B plays a key role. We must caution that eq 8 must necessarily fail when the polymer concentration is high enough to make the assumption of negligible fractional free volume contribution of the polymer invalid. The smaller the molecular weight of the polymer and the higher the temperature, the sooner would this assumption break down.

The limiting value of D_s^* at zero solvent concentration shown in Figure 5 has been extracted from the data by plotting $[\ln (D_s^*/D_0)]^{-1}$ vs. ϕ_2^{-1} for ϕ_2 between 0.45 and 0.75 and then extrapolating the resulting curve to $\phi_2 = 1$. In the infinite solvent dilution limit ($\phi_2 = 1$), the self-diffusion diffusion D_s^* and the mutual cooperative diffusion coefficient D_c must be identical. Although the molecular weight of PBMA in the solutions studied by NMR is different from that of the light scattering experiments, we assume that the self-diffusion of solvent molecules and the binary cooperative diffusion coefficient are independent (or weakly dependent) of the polymer molecular weight.[11]

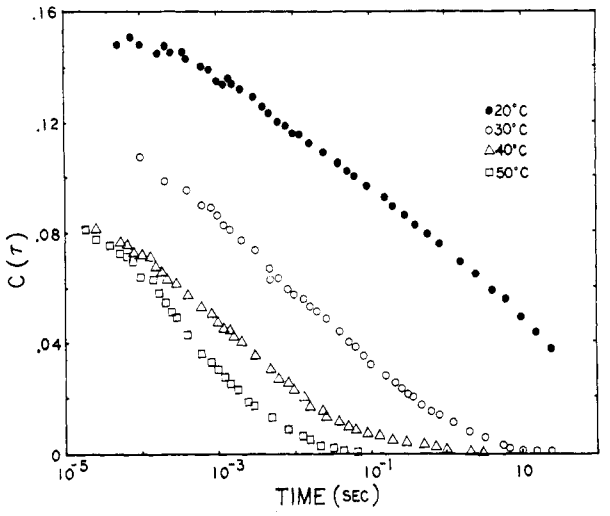

Figure 11. Plots of composite correlation functions for bulk PBMA at four different temperatures.

D. Relaxations of Polymer Melts. We have examined the photon correlation results of pure PBMA melts as a function of temperature near and above its glass transition temperature ($T_g \approx 20$ °C). As schematically indicated in Figure 1 for $\phi = 1$, the slowest internal mode relaxation times could lie beyond the correlator's time limit. This is the case for the correlation observed at 20 °C shown in Figure 11, which indicates an extremely wide distribution of relaxation times spanning more than 8 decades of time scales. These correlations are obtained by matching photon correlations obtained with different time delays into composite correlations covering a wide spread in time. Very wide distributions of relaxations observed by photon correlation near T_g have been previously reported for polystyrene.[5] The preparation of a good pure PBMA sample for light-scattering purposes had until now presented some difficulties due to built-in strains and inhomogeneities during the preparation. Our preparation procedure seems to be quite successful since we have achieved a Landau–Placzek ratio of ~2.0, indicating a nearly perfectly homogeneous sample.[31] For temperatures above T_g, the slowest internal relaxation modes move into the correlator window and the observed correlations at 30, 40, and 50 °C decay down completely to a base line within the time regime of our correlator at the expense of the fastest part of the relaxation distribution lost beyond the shortest time delay. All the correlation functions observed on the melt were independent of the scattering angle. The effect of the addition of a solvent on the relaxation spectrum of polymer melts has often been considered to be equivalent to the effect of increasing the temperature. While this is in part correct as the whole distribution of relaxations move to faster time scales as indicated in Figure 1, the presence of the solvent leads to the appearance of the cooperative diffusion mode, which is likely to couple with the internal relaxation modes of the polymer and impart a q-dependent character to the photon correlation as observed for the 75% solution in Figure 7. The results of Figure 11 for pure PBMA can be analyzed in terms of the Williams–Watts empirical equation,[17] which has been used to describe the distribution of relaxation in polymer melts.[5] Unlike previously reported results on PBMA,[32] we do not observe any anomalous behavior of the correlation at 50 °C.

Acknowledgment. We are grateful to M. Birnboim for many discussions concerning the Birnboim correlator and its use in the photon correlation experiment. We are also grateful to S. M. Lindsay for kindly providing us with Landau–Placzek ratios for some of our samples. Financial support for the light-scattering equipment was provided by the Research Corp. and a Du Pont young faculty grant. The research was supported by NSF Grant DMR 81-11114 of the Polymers Program.

Registry No. PBMA (homopolymer), 9003-63-8; MEK, 78-93-3.

References and Notes

(1) (a) Mathiez, P.; Weisbuch, G.; Mouttet, C. *Biopolymers* **1979**, *18*, 1465. (b) Mathiez, P.; Mouttet, C.; Weisbuch, G. *J. Phys. (Paris)* **1980**, *41*, 519.
(2) (a) Reihanian, H.; Jamieson, A. M. *Macromolecules* **1979**, *12*, 684. (b) Chu, B.; Nose, T. *Ibid.* **1980**, *13*, 122. (c) Nishio, I.; Wada, A. *Polym. J. Jpn.* **1980**, *12*, 145.
(3) (a) Amis, E. J.; Han, C. C. *Polymer* **1982**, *23*, 1403. (b) Amis, E. J.; Janmey, P. A.; Ferry, J. D.; Yu, H. *Macromolecules* **1983**, *16*, 441. (c) Chang, T.; Yu, H. *Macromolecules* **1984**, *17*, 115.
(4) (a) Brown, W.; Johnsen, R. M.; Stilbs, P. *Polym. Bull.* **1983**, *9*, 305. (b) Brown, W. *Macromolecules* **1984**, *17*, 66.
(5) Lindsey, C. P.; Patterson, G. D.; Stevens, J. R. *J. Polym. Sci.* **1979**, *17*, 1547.
(6) Ferry, J. D. "Viscoelastic Properties of Polymers", 3rd ed.; Wiley: New York, 1980; Chapter 17.
(7) Fujita, H. *Fortschr. Hochpolym.-Forsch.* **1961**, *3*, 1.
(8) See, for example: Yamakawa, H. "Modern Theory of Polymer Solutions"; Harper and Row: New York, 1971.
(9) Amis, E. J.; Han, C. C.; Matsushita, Y. *Polymer*, in press.
(10) Brown, W., private communication.
(11) de Gennes, P.-G. "Scaling Concepts in Polymer Physics"; Cornell University Press: Ithaca, NY, 1979.
(12) Bearman, R. J. *J. Phys. Chem.* **1961**, *65*, 1961.
(13) DeGroot, S. R.; Mazur, P. "Non-Equilibrium Thermodynamics"; North-Holland Publishing Co.: Amsterdam, 1962; Chapter 11.
(14) Bearman, R. J.; Kirkwood, J. G.; Fixman, M. *Adv. Chem. Phys.* **1958**, *1*, 1.
(15) Berne, B. J.; Pecora, R. "Dynamic Light Scattering with Applications to Chemistry, Biology, and Physics"; Wiley: New York, 1976.
(16) Fytas, G.; Meier, G.; Patkowski, A.; Dorfmüller, Th. *Colloid Polym. Sci.* **1982**, *260*, 949.
(17) Hwang, D. H. Ph.D. Thesis, Cornell University, 1984.
(18) Crank, J.; Park, G. S. "Diffusion in Polymers"; Academic Press: New York, 1968.
(19) Vrentas, J. S.; Duda, J. L. *J. Polym. Sci., Polym. Phys. Ed.* **1977**, *15*, 441.
(20) Geissler, E.; Hecht, A. M. *J. Phys. Lett.* **1979**, *40*, L-173.
(21) Leger, L.; Hervet, H.; Rondelez, F. *Macromolecules* **1981**, *14*, 1732.
(22) Van Geet, A. L.; Adamson, A. W. *J. Phys. Chem.* **1964**, *68*, 238.
(23) (a) Cosgrove, T.; Sutherland, J. M. *Polymer* **1983**, *24*, 534. (b) Brown, W.; Stilbs, P.; Johnsen, R. M. *J. Polym. Sci., Polym. Phys. Ed.* **1983**, *21*, 1029.
(24) Yu, T. L.; Reihanian, H.; Jamieson, A. M. *Macromolecules* **1980**, *13*, 1590.
(25) Brown, W.; Stilbs, P.; Johnsen, R. M. *J. Polym. Sci., Polym. Phys. Ed.* **1982**, *20*, 1771.
(26) Vrentas, J. S.; Duda, J. L. *J. Polym. Sci., Polym. Phys. Ed.* **1977**, *15*, 403.
(27) Paul, C. W. *J. Polym. Sci., Polym. Phys. Ed.* **1983**, *21*, 425.
(28) Doolittle, A. K. *J. Appl. Phys.* **1951**, *22*, 1471.
(29) Mackin, D.; Rogers, C. E. *Makromol. Chem.* **1972**, *155*, 269.
(30) Hsu, T. P.; Ma, D. S.; Cohen, C. *Polymer* **1983**, *24*, 1273.
(31) Patterson, G. D.; Latham, J. P. *J. Polym. Sci., Macromol. Rev.* **1980**, *15*, 1.
(32) Jamieson, A. M.; Simha, R.; Lee, H.; Tribone, J. *J. Polym. Eng. Sci.* **1981**, *21*, 965.